Introduction to Plasma Research at Occidental College

I. INTRODUCTION

Plasma transport, and neoclassical transport in particular, are topics of great interest in plasma physics, but these topics are difficult to study in a fundamental way. Non-neutral plasma traps are well suited to this task because the intrinsic transport is low and induced transport can thus be studied in a controlled manner. The work at Occidental College is a primarily experimental program of research on radial transport of electrons in a non-neutral plasma trap. In particular, we have studied transport produced by applied asymmetric fields.

The experiments were performed on a modified Malmberg-Penning trap at Occidental College. This device has unique features which allow us to avoid complications we have previously encountered in such research. Specifically, the plasma density has been lowered by a factor of 100 so as to minimize collective contributions to the applied asymmetric field. The azimuthal $E \times B$ drift normally produced by the plasma self-field is provided by a biased wire running axially down the center of the trap. Previous confinement experiments on this trap show the same parameter scaling as observed in higher density plasmas, thus validating our approach. Forty wall sectors are used to create the asymmetric field, thus reducing the number of Fourier modes applied to the plasma and simplifying comparisons to theory.

II. SCIENTIFIC BACKGROUND

The research performed at Occidental College is closely related to current and previous work on the confinement of non-neutral plasmas. Some of this research is reviewed here in order to provide a background for our work. The logic and methods of our work are best understood in light of previous work on radial transport in these systems.

A. Non-neutral Plasmas.

Non-neutral plasmas have unique and interesting properties which make them especially suitable for basic plasma physics research and for various applications. Typically these

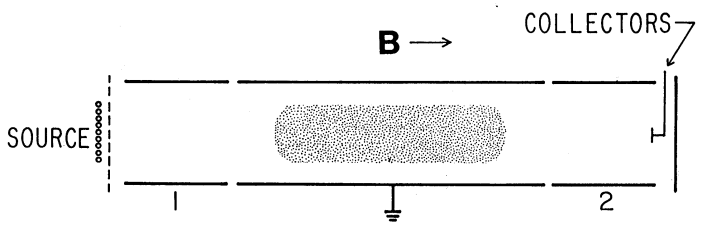

FIG. 1: Schematic of simple non-neutral plasma trap (from Ref. [3])

plasmas are contained in cylindrical geometry, with an axial magnetic field providing radial confinement and applied end potentials providing axial confinement – the so-called Malmberg-Penning Trap [1, 2]. The conducting wall is divided into three (or more) sections, with the plasma normally residing in the grounded central section (see Fig. 1). For electron traps, the end sections are biased sufficiently negatively that axial confinement of the electron plasma is assured. Typical parameters for electron plasmas are: density $n_0 = 10^7$ cm^{-3}, electron thermal energy $kT = 1$ eV, and magnetic field $B =$ several hundred gauss (for non-superconducting coils). The plasma is rotating, since the radial electric field due to space charge gives an $E \times B$ drift in the θ direction. The plasma is typically both stable and reproducible.

B. General Transport Issues.

Theoretically, the radial transport of such a plasma is constrained by conservation of the total canonical angular momentum [4]:

$$P_\theta = \sum_j \left[m v_{\theta j} r_j + (q_j/c) A_\theta(r_j) r_j \right] . \tag{1}$$

Here, (r, θ, z) are cylindrical coordinates, and the vector potential is given by $A_\theta(r) = Br/2$, neglecting the diamagnetic field which is small compared to B for the low densities and low electron velocities considered here. The confinement is easiest to understand for the case where B is sufficiently large that we may ignore the first term. In this case we have $P_\theta \approx (qB/2c) \sum r_j^2$. Thus, in the absence of external torques, the plasma cannot change its mean square radius and there can be no bulk radial expansion of the plasma.

Of course, in actual containment devices there are always effects which can change the angular momentum of the plasma, causing plasma expansion, heating, and loss. Two im-

portant examples of such effects are electron-neutral collisions and electric or magnetic fields that are not cylindrically symmetric. Transport due to electron-neutral collisions has been previously studied [2] and was found to agree in detail with theoretical predictions [5] for neutral pressures above 10^{-7} Torr. More recent work [6] on transport due to electron-neutral collisions is also consistent with classical theory. As the neutral pressure is lowered below 10^{-7} Torr, however, it was found [7] that the confinement of long plasmas was much worse than that expected from electron-neutral collisions. This anomalous loss is believed to be caused by small electric and magnetic field asymmetries due to construction imperfections. Experiments by Driscoll, Malmberg, and Fine [8, 9] established that this anomalous loss depends strongly on the length L of the plasma column and on the axial magnetic field (scaling as L^2B^{-2}).

C. Transport Due to Applied Asymmetries.

Efforts to understand this anomalous transport have involved measuring the net change in the radial density profile produced by *applied* field asymmetries. These asymmetric fields can be produced, for example, by applying various voltages to azimuthally divided conducting walls of the non-neutral plasma trap. The asymmetric potential produces an E_θ and thus a radial $E \times B$ drift which leads to a net expansion of the plasma. It is easy to produce and measure this transport, and several experimenters have worked on this problem [10–18], but a solid connection between experiment and theory is lacking.

Conceptually, it is useful to divide the asymmetry-induced transport problem into two parts: 1) determine the asymmetric field in the plasma and 2) determine the transport produced by these fields. The key features of the Occidental trap are motivated by our previous work showing that part 1) can be quite complex and can interfere with attempts to understand the transport.

1. Determining Asymmetric Fields: Previously Encountered Problems.

While it is easy to apply asymmetric potentials to the walls of a non-neutral plasma trap, our previous work [3, 10, 19] has shown that it is not always easy to determine the plasma's response to these wall potentials. These potentials cannot be directly measured with probes

since anything inserted into the plasma would degrade its confinement. Thus we are faced with calculating the potentials using plasma theory. There are two issues here: the number of spatial Fourier modes produced by a localized wall potential and the plasma's response to these modes. We consider each of these in turn.

Determining the plasma's response to wall potentials involves solving Poisson's equation. As usual in plasma theory, the equation is linearized to make it tractable, and the equation is solved for a Fourier mode having the form $\phi(r)\exp[i(\omega t - kz - l\theta)]$ where ω is the frequency of the field asymmetry and l and k are the azimuthal and axial Fourier wavenumbers of the asymmetry. In order to apply the boundary conditions at the wall, the wall potential must also be broken up into Fourier modes. Since the wall potentials are localized, many Fourier modes are produced. While this involves much algebra, the process is straightforward. However, there are two reasons to minimize the number of these modes. First, in a quasilinear transport theory each of these modes will produce a term in the flux equation: $\Gamma_{theory} = \Gamma_1 + \Gamma_2 + \Gamma_3 + ...$, whereas in the experiment, the flux is a single number. Since the combination of theoretical terms Γ_i producing a given flux value is not unique, the cleanest comparison between experiment and theory would involve a single Fourier mode. This fact led us to increase the number of wall sectors in our device so as to decrease the number of modes.

A second reason to increase the number of sectors is to ensure that the wall potentials do not get too big. When, as in previous experiments, the potentials are applied with a single cylinder of length L_s , the amplitude of the Fourier modes will be proportional to $(L_s/L)\phi_W$, where L is the length of the entire plasma and ϕ_W is the wall potential. Thus, the smaller L_s/L is, the larger the wall potential will have to be to produce a mode of given amplitude and thus a given amount of transport. However, the amplitude of the wall potential is not unrestricted. Linear theory assumes the trajectories of the electrons do not differ radically from the unperturbed case. Since the potentials in the vicinity of the wall sector are on the order of the wall potential, theory requires $e\phi_W << kT_e$. Thus, in order to satisfy theoretical assumptions while producing an observable amount of transport, many wall sectors are useful.

Now let us turn to the second issue: determining the plasma's response to the applied wall potentials. This, of course, is necessary because it is the field strength in the plasma that determines the transport. Again, the procedure is straightforward, if tedious: having found

the Fourier components of the wall potential (i.e. the boundary conditions), we numerically integrate Poisson's equation for each set of (k, l, ω). Our previous studies have shown, however, that this step at best involves some subtleties and at worst may be impossible. The subtleties are due to the variable plasma response to the various Fourier components of the wall potential. Certain values of (k, l, ω) will produce a potential that falls off rapidly inside the plasma (Debye shielding limit), others values will drive plasma modes, and others will produce a response somewhere in between (for details see reference [20]) When a mode is driven, the collectively enhanced potentials produce enhanced transport [3, 10, 13]. Such enhancements at mode frequencies make it difficult to observe any frequency dependence in the transport part of the problem. The situation is further complicated by the fact that applied field asymmetries can also couple to additional plasma modes *nonlinearly*, e.g. through three-wave processes and induced scattering [19, 21].

These complications can be more than annoying. When a plasma mode is driven, the distribution function at the phase velocity of the mode will determine its amplitude. But this is the same part of the distribution producing the radial transport. Thus, the problem can be inherently nonlinear: the transport depends on the asymmetric potentials in the plasma, but the amplitude of these potentials is sensitively dependent on any modification in the distribution of the resonant particles (i.e. it is dependent on the transport). Clearly, the "easy" part of this problem (determining the fields that lead to transport) is not easy at all. While the physics of these phenomena is interesting, we do not believe it is essential to understanding the transport, and this belief is supported by our results to date. Thus, in our trap we have lowered the density by a factor of 100 to minimize collective contributions to the asymmetric field.

2. Determining the Transport: Resonant Particle Transport Theory.

The second part of the transport problem is to calculate the radial particle flux produced by a known asymmetric field in the plasma. We have adapted [20] the theory of asymmetry-induced transport originally developed to describe non-ambipolar radial losses in tandem mirrors [22, 23] to Malmberg-Penning traps. The basic idea of the resulting resonant particle transport theory is that the radial flux is largely associated with particles that experience a resonance with the asymmetric field. The resonance condition is $\omega - l\omega_R - kv_z = 0$, where ω

is the frequency of the field asymmetry (for static fields $\omega = 0$), ω_R is the azimuthal $E \times B$ drift frequency of the plasma column, v_z is the axial velocity, and l and k are the azimuthal and axial Fourier wavenumbers of the asymmetry. The resulting radial particle flux can be written in the form

$$\Gamma = -\sum_{n,l,\omega} \left[D_{nl\omega} \frac{dn_0}{dr} + n_0 V_{nl\omega} \right] \tag{2}$$

where $D_{nl\omega}$ and $V_{nl\omega}$ are related by a generalization of the Einstein relation

$$V_{nl\omega} = \frac{r\omega_c}{l\overline{v}^2}(\omega - l\omega_R) D_{nl\omega} = \sqrt{2}\frac{n\pi}{L}\frac{r\omega_c}{l\overline{v}} x D_{nl\omega}. \tag{3}$$

The function $D_{nl\omega}$ assumes various forms depending on the strength and nature of the resonance, the vicinity of additional resonances, and the relative importance of collisions. The simplest of these corresponds to the case of an asymmetry which is sufficiently weak that the trapping frequency is small compared to the effective collision frequency (the plateau regime):

$$D_{nl\omega} = \frac{1}{\sqrt{2\pi\overline{v}^2}} \frac{L}{|n|} \left| \frac{cl\phi_{nl\omega}(r)}{rB} \right|^2 e^{-x^2}. \tag{4}$$

This function is modified when the strength of the interaction is such that the trapping frequency is larger than the effective collision frequency (banana regime). We then obtain

$$D_{nl\omega} = \frac{1}{\sqrt{2\pi}} \frac{\nu \left(\frac{L}{n\pi}\right)^2 \left(\frac{l\overline{v}}{r\omega_c}\right)^2 \left(\frac{e\phi_{nl\omega}(r)}{T}\right)^{1/2}}{\left[1 - \left(\frac{lL}{n\pi}\right)^2 \frac{1}{r\omega_c}\frac{d\omega_R}{dr}\right]^{3/2}} e^{-x^2}. \tag{5}$$

For simplicity, we have assumed here that the temperature T is constant with radius. The variable x is equal to $v_{res}/\sqrt{2}\,\overline{v}$, where $v_{res} = L(\omega - l\omega_R)/n\pi$ is the resonant velocity for the asymmetry mode n, l, ω (n is the axial mode number kL/π). The symbols n_0, $\overline{v}$, ω_c, and ν_{ee} denote the electron density, thermal velocity, cyclotron frequency, and the electron-electron collision frequency, respectively. $\phi_{n,l,\omega}$ is the Fourier mode amplitude associated with asymmetry mode (n, l, ω) and includes any collective response of the plasma to the wall voltages. The remaining quantities have been previously defined or are standard notation. Note that, as we claimed earlier, the flux involves a sum over all Fourier modes present. Also, the dominance of the transport by resonant particles is reflected in the e^{-x^2} term, which is the Maxwellian distribution function evaluated at the resonant velocity. A third regime occurs when neighboring resonances overlap and the transport becomes independent of collisions (stochastic regime).

It is important to note that, since the trapping frequency depends on the amplitude of the field asymmetry in the plasma, one must know this amplitude to determine which transport regime describes the experiment. This is yet another reason to minimize collective contributions to the asymmetric field.

It is clear that collective processes can play an important role in these experiments. The linear and nonlinear processes observed experimentally [10, 19] can change the magnitude of the transport by significant amounts. However, it is not clear that collective processes play an essential role in determining the nature of the transport. If our two-part division of the transport problem is correct, then the main role of collective effects is to alter the amplitude of asymmetric fields in the plasma. In this case their presence only complicates the experiment and may well mask other fundamental processes.

III. THE OCCIDENTAL COLLEGE TRAP

The research program at Occidental College seeks to explore radial transport in the absence of collective effects. Our experimental device has been designed to avoid the difficulties outlined in part II C so that we can focus on understanding the transport. First, in order to minimize the number of Fourier modes we have divided our confinement region into forty sections (five cylinders with eight azimuthal divisions each). Of course, more is better with regard to the number of these sections, but this number can be reasonably handled and is a great improvement over other experiments having at most eight sections. Secondly, in order to simplify the task of determining the potentials in the plasma we have reduced the plasma density by at least a factor of 100 and increased the plasma temperature. These changes increase the Debye length to the point where collective effects are minimized (since both Debye shielding and mode damping depend sensitively on the Debye length). Thus the potentials in the plasma should be close to the vacuum potentials. The radial electric field formerly produced by the plasma column is now provided by a negatively biased wire running along the axis of the trap. Thus the basic dynamical motions of electrons in our trap are the same as in any other (axial bounce motion and azimuthal drift motion). In essence, we have constructed a trap where the electrons will act as test particles moving in prescribed fields.

The apparatus for our experiments is shown schematically in Fig. 2. A gold-plated copper

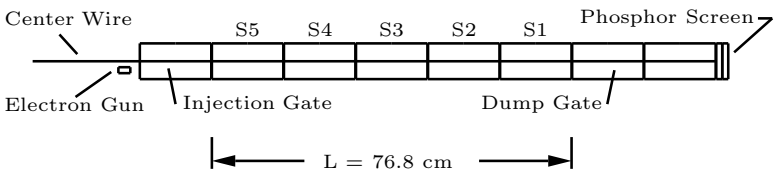

FIG. 2: Schematic of the Occidental College Trap. The usual plasma column is replaced by a biased wire to produce the basic dynamical motions in low density electrons injected from an off-axis gun. The low density and high temperature of the injected electrons largely eliminate collective modifications of the vacuum asymmetry potential. The five cylinders (labeled S1 through S5) are divided azimuthally into eight sectors each.

tube with 3.05 in. I.D. is divided into eight electrically isolated parts, each 6.00 in. long. Five of these (labeled S1 - S5) are further divided azimuthally into eight equal sectors to allow for experiments with applied electric field asymmetries. An electrically isolated 0.014 in. diameter wire runs along the axis of the device. This electrode structure is positioned along the axis of the main vacuum chamber and the entire device is placed in a long solenoid which provides a uniform magnetic field variable over the range 0 - 600 gauss. Cancellation of the earth's magnetic field and fine alignment of the electrode and solenoid axes is provided by two sets of "bent head" rectangular magnetic field coils. The base vacuum pressure is 3.5×10^{-10} Torr and the residual gas consists mainly of hydrogen.

The experiment runs in cycles with a timing sequence as follows. Two of the electrodes are used as injection and dump gates which are normally held at a large negative potential (typically -140V). The remaining cylinders are grounded. The center wire is also normally at a selected bias (-140 to +140V). To start a cycle the bias on the center wire is set to zero. We then ground the injection gate and apply a negative pulse (1.0 to 12.0V) to an off-axis electron gun cathode (cf. Fig. 2). After the gun is pulsed, the injection gate is returned to a negative potential and the center wire is switched first to -140V for 100 μs and then to the selected final bias level. The electrons are now trapped between injection and dump gates and are held for a variable time during which transport-producing asymmetries are applied to some or all of the forty wall sectors. Finally, the dump gate is grounded, allowing the remaining electrons to escape axially along magnetic field lines and hit a positively-biased phosphor-coated screen. If one wishes to change the length of the confinement region, the role of injection gate and dump gate may be assigned to other sections of the trap.

The phosphor screen serves two diagnostic purposes: 1) as a collection plate, it provides a measurement of the total charge remaining in the machine at the dump time. 2) If the bias on the screen is increased sufficiently, the phosphor will emit light. These phosphor screen images show the spatial distribution of the electrons and thus, along with the measurement of the total charge, allow a computation of the electron density. The image data is obtained with a sensitive, computer controlled CCD camera with up to sixteen bits of dynamic range. It is also possible to analyze electrons escaping from partial dumps (i.e., the dump gate made less negative but not grounded) to obtain the axial distribution function of the electrons [24].

The electrons from the gun initially form a small-radius off-axis column with a typical peak density of 10^7 cm^{-3}. However, the strong adverse radial shear in the $E \times B$ velocity produced by the high initial negative bias on the center wire quickly disperses the electrons. Within 100 μs the electrons have reached a symmetric annular distribution with a peak density reduced to 10^5 cm^{-3}. Details are given in reference [25]. Since the time for particle loss to the walls is much larger than this, we can ignore the details of this initial rearrangement and take the symmetrically filled device as our initial condition. The electron density at this point is low enough that its contribution to the radial electric field is negligible for typical center wire potentials. The reduced density together with increased axial temperature (typically 4 eV) gives a Debye length 4.7 cm. This is larger than our wall radius (3.87 cm) and 20 times larger than a typical pure electron plasma (density 10^7 cm^{-3}, temperature 1 eV, Debye length 0.23 cm). Although our Debye length is still small compared to the machine length, there is no point in decreasing it further since even vacuum potentials fall off axially with a scale length equal to the radius of the conducting wall.

In order to apply the simplest asymmetry possible we generally use all forty wall sectors and apply to each a signal with proper amplitude and relative phase. These wall potentials are provided by two Pragmatic 2205A arbitrary waveform generators with a common clock generator. Each of these devices provides two channels of phase-locked, variable frequency sine-wave (up to 10 MHz). These four channels go into power splitters which give an in-phase and a 180-degree out-of-phase output, thus providing the eight signals for the eight azimuthal wall divisions (for example, for an $l = 1$ asymmetry relative phases of 0, 45, 90, 135, 180, 225, 270, and 315 degrees are used). These signals are then attenuated as needed to provide the axial variation in wall potentials. These potentials are gated on after the electrons are injected and gated off just before they are dumped. On subsequent experimental cycles,

the frequency, amplitude, or phase of the sine-waves can be adjusted as needed. The entire experiment is computer-controlled so that parameter space can be scanned automatically.

We note that all of the significant parameters in this experiment are independently adjustable. These include the axial magnetic field, the radial electric field, the asymmetry field strength, the frequency ω and Fourier mode numbers (l, k), the machine length, and the axial electron velocity. This allows for a complete investigation of the relevant parameter space. The azimuthal rotation frequency ω_R is also easily adjustable:

$$\omega_R = \frac{-\phi_{cw}}{r^2 B \ln(R/a)} \tag{6}$$

where ϕ_{cw}, R, and a are the center wire bias and the radii of the wall and the center wire, respectively.

This system has several advantages. Since there are no collective effects, the asymmetric fields may be easily calculated given the wall potentials, and the calculated fields will vary in a known way (i.e. linearly) with the wall potentials. The drift frequency ω_R and the parallel velocity v_z, which are fundamental parameters in the transport theory, are independently variable over a large range (electron contribution to ω_R is negligible). Finally, the phosphor screen readout of particle position allows for greater spatial resolution than is practical with particle collectors.

The reduction of density in our trap should also decrease the electron-electron collision frequency, and it might be argued that this is a significant difference between our experiment and higher density electron plasmas. However, our previous work suggests that this is not the case. We have studied the scaling of confinement time in our device (with no applied asymmetry) as a function of machine length L and axial magnetic field B. We found that our confinement time follows the same $(B/L)^2$ scaling found in higher density plasmas, and that, for the same L and B, the absolute confinement time is comparable (see reference [26]). This interesting but puzzling result indicates that the transport process is similar in both cases and that it cannot depend critically on electron density.

IV. SELECTED RESULTS

We now review a few of our results. These results show that resonant particle transport theory is not the correct model for asymmetry-induced transport and suggest an alternative

model.

A. Frequency Dependence of the Transport.

As we have discussed, our unique experimental approach allows us to investigate the frequency dependence of the transport while avoiding the dominating frequency dependence of collective effects (i.e., standing waves). While our experiments on the frequency dependence of asymmetry-induced transport[27, 28] give some superficial support to resonant particle theory, a more detailed examination of the data reveals fundamental discrepancies. A typical experimental signature from these experiments is shown in Fig. 3a where we we plot the measured radial flux Γ vs. asymmetry frequency f at four radial positions. The radial density profile is shown in the inset. As the asymmetry frequency $\omega = 2\pi f$ is varied, the resonant velocity $v_{res} = \frac{L}{n\pi}(\omega - l\omega_R)$ is swept through the electron distribution function and a peak in the transport flux is expected. According to theory [see Eqs. (2) thru (5)], when the density gradient is large, the flux should vary like e^{-x^2}. Since $x = v_{res}/\sqrt{2\overline{v}}$, this is a Gaussian curve centered where $\omega = l\omega_R$. This behavior is shown by the curves for r/R equal to 0.19, 0.30, and 0.55. Note that the sign of the flux changes with the density gradient sign and that the value where $\omega = l\omega_R$ decreases with radius [see Eq. (6)]. At the top of the density profile the gradient is zero, so we expect an xe^{-x^2} behavior, and this seems to match the $r/R = 0.38$ curve. We have verified that the curves shift horizontally in a qualitatively appropriate way when the center wire bias or the magnetic field (and thus ω_R) is varied. Also, if the asymmetry is made to spin opposite the direction of ω_R (corresponding to a resonant velocity further out on the tail of the distribution function), no peaks are observed in the flux, as expected.

Thus, at first glance our experiments seem to support resonant particle theory. However, when we make more detailed comparisons to the predictions of the theory we find serious discrepancies. A typical case is shown in Fig. 3b. Here we have plotted the frequency at which the flux is an extrema, f_{peak}, versus radius and compared with the predictions of resonant particle theory. Note that the decrease of the frequency of the peak flux with radius does not match that given by theory, except for flux minima around $r/R = 0.4$. Even more dramatically, for most radii the predicted flux maxima should occur at negative frequencies (i.e, backward rotation), but the experimental points are all at positive frequencies.

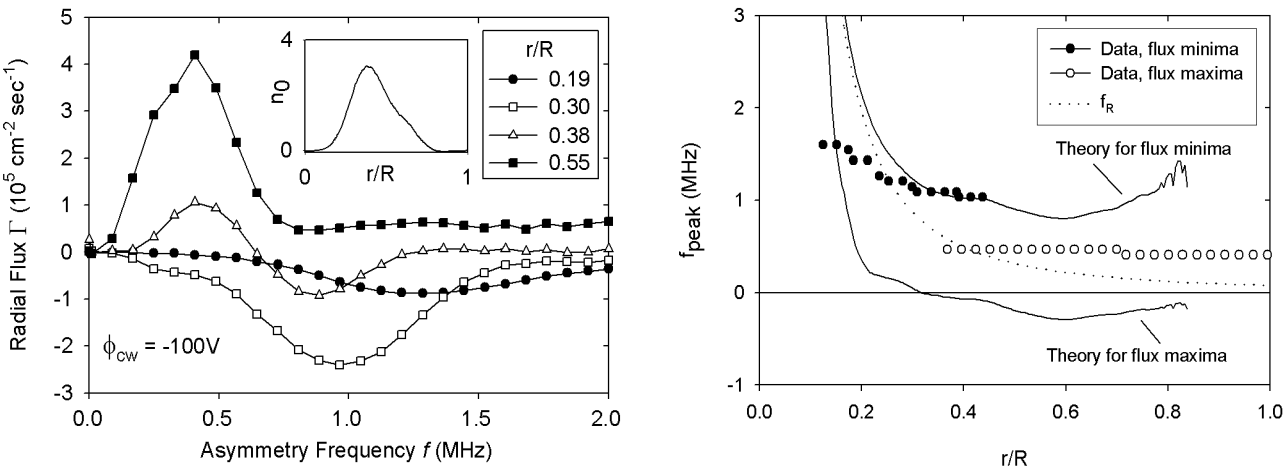

FIG. 3: Frequency dependence of the transport. a) On the left we show the radial particle flux at four selected radii as a function of asymmetry frequency for center wire bias $\phi_{cw} = -110V$, magnetic field $B = 364G$, and Fourier mode numbers $n = 1$, $l = 1$. The shape of the flux curves is qualitatively consistent with that expected from theory. The electron density n_0 (10^5 cm^{-3}) versus scaled radius r/R is shown in the inset. b) On the right we give a comparison of experimental and theoretical values for f_{peak} showing the quantitative discrepancy, and, for the flux maxima, the failure to even get the sign right. Experimental data is shown for the case where B = 364G, ϕ_{cw} = -146V, $n = 1$, and $l = 1$. Experimental density profiles are used to produce the theory curves shown by the solid lines. The rotation frequency f_R is shown by the dotted line for comparison.

A more subtle discrepancy has to do with transport at low frequencies. As shown in Fig. 3a, the experimental flux versus frequency curves always fall to very small values as the frequency approaches zero. This behavior is observed for a wide range of experimental parameters. In contrast, in resonant particle theory there is nothing special about zero frequency and the flux versus frequency curves go smoothly through $\omega = 0$ and extend into negative frequencies. We believe that this discrepancy is an important clue to the transport mechanism. It is worth noting that this discovery stems from our experiment's unique ability to probe the frequency dependence of the transport.

The nature of these discrepancies (large qualitative differences rather than small quantitative differences) suggests that something fundamental is missing from the theory. The focus of our research has thus turned from testing resonant particle transport theory to identifying and elucidating these missing elements.

B. A New Approach to Determining the Magnetic Field Scaling of the Transport

A key experimental signature for transport is the scaling with magnetic field. We have developed[29, 30] a new approach to finding the magnetic field scaling of the asymmetry-induced radial flux Γ and the results also contradict resonant particle transport theory. Our approach is based on the observation that the magnetic field B enters the transport physics in at least two ways. Firstly, in the zeroth order azimuthal $E \times B$ drift produced by the radial electric field $v_\theta = E_r/B$. This causes the particle guiding centers to drift around the trap axis with angular frequency $\omega_R = v_\theta/r$. Secondly, the magnetic field enters in the first order radial $E \times B$ drift produced by the applied asymmetry $v_r = E_\theta/B$. It is this drift which is responsible for the radial transport of particles and is thus most fundamental to our study.

Our new experimental technique removes the ω_R dependence and thus isolates the remaining first order magnetic field dependence. The technique is based on the hypothesis that the asymmetry frequency ω and the plasma rotation frequency ω_R always enter the transport physics in the combination $\omega - l\omega_R$, where l is the azimuthal mode number of the applied asymmetry. We then select from a Γ vs r vs ω data set those points where $\omega - l\omega_R = 0$, thus insuring that any function of this combination is constant. When the selected flux Γ_{sel} is plotted versus the density gradient ∇n_0, a roughly linear dependence is observed, showing that this selected flux is diffusive. This linear dependence is roughly independent of the bias of the center wire in our trap ϕ_{cw}. Since in our experiment ω_R is proportional to ϕ_{cw}, this latter point shows that our technique has successfully removed any dependence on ω_R and its derivatives, thus confirming our hypothesis. The slope of a least-squares fitted line through the Γ_{sel} vs ∇n_0 data then gives the diffusion coefficient D_0 under the condition $\omega - l\omega_R = 0$. Varying the magnetic field, we found that D_0 is proportional to $B^{-1.33}$, a scaling that does not match either regime of resonant particle transport theory.

We have also used an extension of this technique (examining data points adjacent to the $\omega - l\omega_R = 0$ point) to constrain the form of the empirical flux equation, thus providing a touchstone for future model development[31]. One of the interesting results is that the mobility part of the transport is much smaller than predicted by the Einstein relation Eq. (3).

C. Single-Particle Simulations

As noted above, it appears that resonant particle transport theory does not give a correct description of asymmetry-induced transport. As an additional investigative tool, we have developed a single-particle computer simulation to study the dynamics of particles moving in prescribed asymmetric fields. The results[32] were surprising and indicate that there are important particle dynamics not included in resonant particle theory. A representative result is shown in the contour plots of Fig. 4. The plots show the maximum radial excursion of particles as a function of their initial velocity v_z and radial position r/R. The plot on the left is for a helical asymmetry with periodic boundary conditions in the axial direction. The superimposed solid line shows the position of the resonant velocity $v_{res} = L(\omega - l\omega_R)/n\pi$ and the dashed lines show the theoretical width of the resonance, which is set by the usual banana regime orbits of particles trapped in the moving potential of the wave. These match the simulation perfectly. This particular example is for $\omega = 0.5 \times 10^6$ rad/s. For higher (lower) frequencies, the zero-crossing of the curve would shift to the left (right).

In experiments, however, particles reflect at the ends and the usual asymmetry is a standing wave. Under these conditions we obtain the plot on the right. Now there are two resonances, one for each of the counter-propagating helical waves that make up the standing wave. When the two resonances overlap, however, the particle dynamics are not just the sum of the individual wave dynamics. Rather, the particle motion becomes *stochastic* with a much larger group of particles undergoing large radial excursions. Interestingly, there is no threshold for the appearance of this stochastic regime; it will always be present where the two resonances cross. Furthermore, at the core of this stochastic region (around $v_{res} \approx 0$) is a group of particles that have especially large radial excursions. Additional studies show that these particles reflect off the asymmetry potential and are *axially trapped in the lab frame*. This axially trapping is distinct from the usual banana regime trapping in the wave frame.

It is important to note that this new process has features that are quite different from resonant particle transport. The process occurs only near the radial location where $v_{res} = 0$ or, equivalently, where $\omega = l\omega_R$. This might explain the anomolously low transport we observe at low frequencies (see section IV A) since this condition cannot be satisfied for frequencies lower than the value of $l\omega_R$ at the wall. Also, this process only involves low

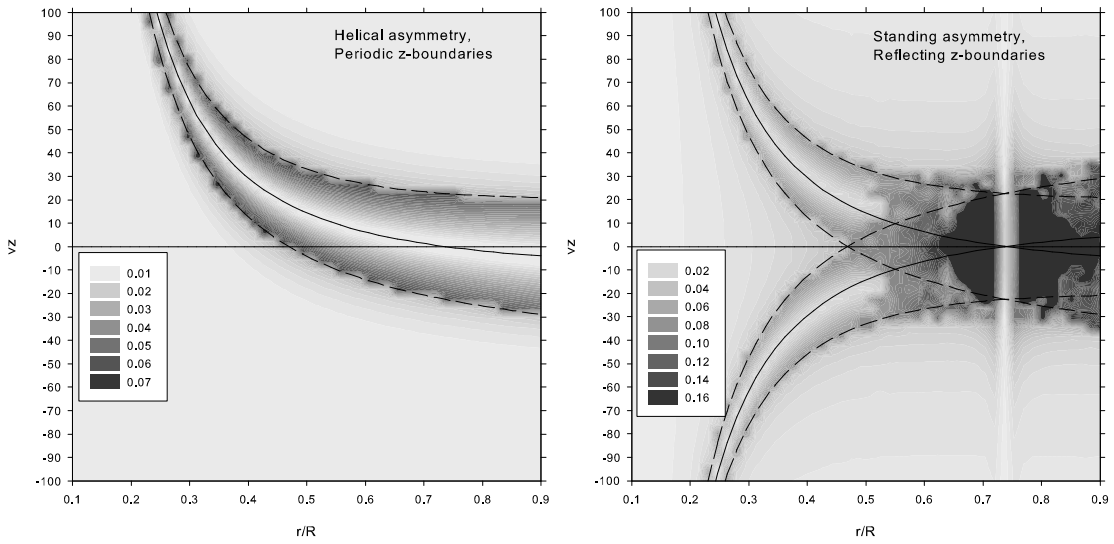

FIG. 4: Single particle simulation results for typical experimental conditions. The shading shows the value of the maximum radial excursion $\Delta r/R$ as a function of initial velocity v_z and radial position r/R. Note the $\Delta r/R$ scale is different for the two plots. The left plot shows the case of a helical asymmetry with periodic boundary conditions while the right plot is for a standing wave with reflecting boundaries. The asymmetry frequency is $\omega = 0.5 \times 10^6$ rad/s and v_z has units of 10^6 cm/s.

velocity particles, whereas resonant particle transport can occur for any velocity satisfying the resonance condition. This feature might explain why plasma heating reduces transport in "rotating wall" experiments[16–18].

More recently, we have added collisions to our code, thus allowing us to determine the transport coefficients for comparison to analytical theory and experiments[33]. We were able to show agreement between the simulation and resonant particle theory for the simplest case, but found that, generally, both resonant particles and axially trapped particles (ATPs) contribute to the transport, and that the latter usually dominate for typical experimental conditions. Although there is no analytical theory for ATP transport, we have had some success explaining the simulation results using a heuristic transport model[34].

One intriguing result from this work is that, for ATP transport, the mobility part is much larger than predicted by the Einstein relation Eq. (3). The failure of the Einstein relation is not surprising given the non-equilibrium nature of the ATPs. As noted above, however, the

experiment indicates that the mobility part is much *smaller* than predicted. This striking discrepancy is not understood, but we suspect it may be resolvable by taking into account the non-local nature of the transport produced by ATPs with large radial excursions. The need for such a modification has previously been noted by researchers studying transport in neutral plasmas[35–37].

---

[1] J. H. Malmberg and J. S. deGrassie, "Properties of Nonneutral Plasmas", Phys. Rev. Lett. **35**, 577 (1975).

[2] J. S. DeGrassie and J. H. Malmberg, "Waves and Transport in the Pure Electron Plasma", Phys. Fluids **23**, 63 (1980).

[3] J. H. Malmberg, C. F. Driscoll, B. Beck, D. L. Eggleston, J. Fajans, K. Fine, X.-P. Huang, and A. W. Hyatt, "Experiments with Pure Electron Plasmas", in Non-neutral Plasma Physics, C.W. Roberson and C.F. Driscoll, editors, (American Institute of Physics, New York, 1988), pp. 28-74.

[4] T. M. O'Neil, "A Confinement Theorem for Nonneutral Plasmas", Phys. Fluids **23**, 2216 (1980).

[5] M. H. Douglas and T. M. O'Neil, "Transport of a Nonneutral Electron Plasma Due to Electron Collisions with Neutral Atoms", Phys. Fluids **21**, 920 (1978).

[6] Qudsia Quraishi, Scott Robertson, and Bob Walch, "Classical Collisional Diffusion in the Annular Penning Trap", in Non-Neutral Plasma Physics IV, edited by Francois Anderegg, C. Fred Driscoll, and Lutz Schweikhard, (American Institute of Physics, Melville, NY, 2002), pp. 407-415.

[7] J. H. Malmberg and C. F. Driscoll, "Long-Time Containment of a Pure Electron Plasma", Phys. Rev. Lett. **44**, 654 (1980).

[8] C. F. Driscoll and J. H. Malmberg, "Length-Dependent Containment of a Pure Electron Plasma", Phys. Rev. Lett. **50**, 167 (1983).

[9] C. F. Driscoll, K. S. Fine, and J. H. Malmberg, "Reduction of Radial Losses in a Pure Electron Plasma", Phys. Fluids **29**, 2015 (1986).

[10] D. L. Eggleston, T. M. O'Neil, and J. H. Malmberg, "Collective Enhancement of Radial Transport in a Nonneutral Plasma", Phys. Rev. Lett. **53**, 982 (1984).

[11] J. Notte and J. Fajans, "The Effect of Asymmetries on Non-neutral Plasma Confinement", Phys. Plasmas **1**, 1123 (1994).

[12] X. -P. Huang, F. Anderegg, E. M. Hollman, C. F. Driscoll, and T. M. O'Neil, "Steady-State Confinement of Non-neutral Plasmas by Rotating Electric Fields", Phys. Rev. Lett. **78**, 875 (1997).

[13] F. Anderegg, E.M. Hollmann, and C.F. Driscoll, "Rotating Field Confinement of Pure Electron Plasmas Using Trivelpiece-Gould Modes", Phys. Rev. Lett. **81**, 4875 (1998).

[14] E. M. Hollmann, F. Anderegg, and C. F. Driscoll, "Confinement and manipulation of non-neutral plasmas using rotating wall electric fields", Phys. Plasmas **7**, 2776 (2000).

[15] J. M. Kriesel and C. F. Driscoll, "Two Regimes of Asymmetry-Induced Transport in Non-neutral Plasmas", Phys. Rev. Lett. **85**, 2510 (2000).

[16] R. G. Greaves and C. M. Surko, "Inward Transport and Compression of a Positron Plasma by a Rotating Electric Field", Phys. Rev. Lett. **85**, 1883 (2000).

[17] R. G. Greaves and C. M. Surko, "Radial compression and inward transport of positron plasmas using a rotating electric field", Phys. Plasmas **8**, 1879 (2001).

[18] J. R. Danielson and C. M. Surko, "Torque-Balanced High Density Steady States of Single-Component Plasmas", Phys. Rev. Lett. **94**, 035001 (2005).

[19] D. L. Eggleston and J. H. Malmberg, "Observation of an Induced Scattering Instability Driven by Static Field Asymmetries in a Pure Electron Plasma", Phys. Rev. Lett. **59**, 1675 (1987).

[20] D. L. Eggleston and T. M. O'Neil, "Theory of Asymmetry-Induced Transport in a Non-Neutral Plasma", Phys. Plasmas **6**, 2699 (1999).

[21] J. D. Crawford, T. M. O'Neil, and J. H. Malmberg, "Effect of Nonlinear Collective Processes on the Confinement of a Pure Electron Plasma", Phys. Rev. Lett. **54**, 697 (1985).

[22] D. Ryutov and G. Stupakov, "Diffusion of Resonance Particles in Ambipolar Plasma Traps", Sov. Phys. Dokl. **23**, 412 (1978).

[23] R. Cohen, "Orbital Resonances in Nonaxisymmetric Mirror Machines", Comments Plasma Phys. Cont. Fusion **4**, 157 (1979).

[24] D. L. Eggleston, C.F. Driscoll, B.R. Beck, A.W. Hyatt, and J.H. Malmberg, "Parallel Energy Analyzer for Pure Electron Plasma Devices", Phys. Fluids B, **4**, 3432 (1992).

[25] D. L. Eggleston, "Experimental Study of Two-Dimensional Electron Vortex Dynamics in an Applied Irrotational Shear Flow", Phys. Plasmas **1**, 3850 (1994); Erratum: Phys. Plasmas **2**,

1019 (1995).

[26] D. L. Eggleston, "Confinement of Test Particles in a Malmberg-Penning Trap with Biased Axial Wire", Phys. Plasmas **4**, 1196 (1997).

[27] D. L. Eggleston and B. Carrillo, "Frequency dependence of asymmetry-induced transport in a non-neutral plasma trap", Phys. Plasmas **10**, 1308 (2003).

[28] D. L. Eggleston, "Using Variable Frequency Asymmetries to Understand Radial Transport in a Malmberg-Penning Trap", in Non-Neutral Plasma Physics V, edited by M. Schauer et al., American Institute of Physics, 2003, pp. 40-49.

[29] D. L. Eggleston and J.M. Williams, "Magnetic field dependence of asymmetry-induced transport: a new approach", Phys. Plasmas 15, 032305 (2008).

[30] D. L. Eggleston, "Using variable frequency asymmetries to probe the magnetic field dependence of radial transport in a Malmberg-Penning trap", in Non-Neutral Plasma Physics VII, edited by James R. Danielson and Thomas Sunn Pedersen, American Institute of Physics, 2009.

[31] D. L. Eggleston, "Constraints on an empirical equation for asymmetry-induced transport", Phys. Plasmas 17, 042304 (2010).

[32] D. L. Eggleston, "Particle dynamics in asymmetry-induced transport", Phys. Plasmas 14, 012302 (2007).

[33] D. L. Eggleston, "Two sources of asymmetry-induced transport", Phys. Plasmas 19, 042307 (2012).

[34] D. L. Eggleston, "Dependence of enhanced asymmetry-induced transport on collision frequency", Bull. Am. Phys. Soc. 57 (2012), to appear.

[35] B. Ph. van Milligen, R. Sanchez, and B. A. Carreras, "Probabilistic finite-size transport models for fusion: Anomalous transport and scaling laws," Phys. Plasmas **11**, 2272 (2004)

[36] G. Spizzo, R. B. White, S. Cappello and L. Marrelli, "Nonlocal transport in the reversed field pinch," Plasma Phys. Control. Fusion **51**, 124026 (2009).

[37] K. Gustafson, D. del-Castillo-Negrete, and W. Dorland, "Finite Larmor radius effects on nondiffusive tracer transport in a zonal flow," Phys. Plasmas **15**, 102309 (2008)